Control strategy to improve EV range by exploiting hybrid storage units

Simone Barcellona [1*], Davide De Simone [1], Luigi Piegari [1]

[1] Politecnico di Milano - Dipartimento di Elettronica Informazione e Bioingegneria, Piazza Leonardo da Vinci, 32 – I-20133 Milano (Italy)
[*] simone.barcellona@polimi.it;

Abstract: In the past, the diffusion of electric vehicles (EVs) has been hindered by energy storage limits. In fact, these are the reason for the limited EV range and the consequent range anxiety of their drivers. Thanks to constant improvements in storage system technologies over the years, in terms of both energy and power density, lithium ion batteries (LiBs) now guarantee vehicle ranges higher than 150 km for small vehicles. Another important improvement has been achieved by the hybridization of LiBs with other storage technologies such as electric double layer capacitors or lithium ion capacitors. By adding an additional storage unit (ASU) to the EV battery system, the overall efficiency increases, with a consequent gain in the vehicle's expected range. In a previous paper, an optimal sizing procedure was proposed, through which it is possible to calculate the optimal ASU mass that maximizes the EV range for a given vehicle, ambient conditions, and driving cycle, which was considered to be known a priori. In the present work, a real time implementation of the control strategy on which the optimal sizing procedure was based is proposed and analyzed using the results of simulation tests.

1. Nomenclature

p_{dis}	power drawn from the energy storage system
p_{cha}	power injected into the energy storage system
p_{tot}	total power exchanged with the energy storage system
P_{tot}	average value of p_{tot}
p_o	oscillating part of p_{tot}
v	speed of the electric vehicle
a	acceleration of the electric vehicle
α	slope of the road
M	mass of the electric vehicle
M_e	equivalent rotational mass of the electric vehicle
C_D	aerodynamic coefficient
C_V	rolling friction
S	front surface of the electric vehicle
ρ	air density
g	gravitational acceleration
η_{dis}	total discharge efficiency
η_{cha}	total charge efficiency
m_o	optimal sizing mass of the auxiliary storage unit
ΔE_{ASU}	maximum energy variation allowed by the capacity of the auxiliary storage unit
ΔE_{max}	maximum energy variation related to p_{tot}
p_{ASU}	power portion exchanged with the auxiliary storage unit
p_{BAT}	power exchanged with the lithium ion battery
p_t	total instantaneous power required by the traction drive
P_t	moving average of p_t
T_W	window length of the moving average
t	time
G	split coefficient
G_o	optimal split coefficient
SOD	state of discharge of the battery pack
I	battery current
T	temperature

2. Introduction

Nowadays, the development and sale of electric vehicles (EVs) represent a feasible alternative to traditional vehicles equipped with internal combustion engines. Although electric motors have both higher efficiency and power density than internal combustion engines, and they can easily be controlled through power converters, the on-board energy storage system (ESS) represents the main issue and limiting factor preventing the diffusion of EVs. In fact, the ESS limits the achievable vehicle range.

Nevertheless, electrochemical storage systems have recently been improved, ensuring good performances in terms of power and energy density, thus increasing the vehicle range. In particular, lithium ion batteries (LiBs) are the most commonly used technology for the ESSs of EVs. Their energy density is high enough to ensure vehicle ranges higher than 150 km for the smallest EVs on the market. However, the obtained ranges are still not comparable with those of traditional vehicles. Consequently, these vehicle ranges are also the most important issue related to the range anxiety phenomenon [1]. In order to limit range anxiety, vehicle range estimation has been studied [2]–[7].

Even though, as previously stated, LiBs have a high energy density, their power density is relatively low. For this reason, the hybridization of LiBs with other kinds of storage technologies with higher power densities could be the way to improve the overall efficiency of a hybrid energy storage system, and thus increase the vehicle range. The most attractive devices for this application are electric double layer capacitors (EDLCs) and lithium ion capacitors (LiCs). Usually, both of these are referred to using the general term supercapacitors (SCs). Coupling SCs to the battery would make it possible to obtain a hybrid energy storage system offering both high energy density and high power density. In this way, thanks to presence of SCs, it is possible to support LiBs, especially when high peak currents are requested. In fact, during both the fast braking and accelerating phases, high currents can be exchanged with the LiBs, reducing the efficiency and lifetime of the batteries themselves. If SCs are added to the system, the high current peaks can be divided between the two storage systems, decreasing the stress on the LiBs, which will work with lower currents.

In light of the above, one of the best solutions to maximize the efficiency of LiBs could be to provide them an almost constant power. The coupling of LiBs with SCs has been studied and analyzed in several past works [8]–[16]. Moreover, in the literature, it is possible to find three different hybridization topologies for LiBs and SCs: passive, semi-

active, and fully active. The passive topology is the simplest one and consists of the direct connection of supercapacitors and batteries in parallel on the dc bus of the main dc/ac converter. The higher short circuit resistance of the lithium battery pack will naturally extract the demanded power peaks from the supercapacitors. This approach does not introduce additional losses in the power converters, but provides scarce degrees of freedom in terms of control flexibility [17], [18]. In the semi-active topology, the two storage systems are connected to each other using only one dc/dc converter [19], [20]. Finally, in the fully active topology, the LiBs and SCs each have a proper dc/dc converter connected to the main dc/ac converter [21]–[23]. The last solution is the best in terms of performance. Indeed, in this case, it is possible to use the SCs independently from the batteries, and thus, all the energy stored in the SCs can be exploited. On the other hand, this solution requires an additional power converter to better exploit the energy stored in the SCs.

Focusing on the fully active topology, on one hand, it is important to correctly size the SCs to be added to the battery pack. On the other hand, it is important to choose a proper control strategy for the two dc/dc converters that split the total electric power exchanged with the two ESSs in order to improve the performance of the overall system. In particular, it is possible to increase the lifetime of the batteries and the range of the EVs.

Most of the works found in the literature propose control strategies that split the total electric power based on different constraints such as the state of charge limits, maximum charge/discharge currents, and lifetime to increase the lifetime of the batteries. However, there seems to be a lack of consideration given to the kind of driving cycle for the EV, both in the sizing procedure and in the control strategy to increase the EV range.

Nonetheless, the addition of other storage systems to the LiBs yields an increase in the weight of the EV. This is not always acceptable. Moreover, a higher curb weight increases the average power absorbed by the EV itself.

Starting from these assessments, in the previous work [24], the effectiveness of adding an auxiliary storage unit (ASU) such as a SC to the batteries was assessed. The analysis performed took into account both the weight increase and range extension for different driving cycles, different temperatures, and different EVs. A procedure was proposed that made it possible to find the optimal size for the ASU, in terms of the mass and maximizing the range extension of an EV, with the driving cycle known a priori.

The main difference between the proposed sizing procedure and other past works was the use of the a priori knowledge of the driving cycle to optimize the power splitting between the two ESSs in a simple way. The particularity was given by the fact that the proposed sizing procedure was related to the control strategies to be used. The main issue in a real time implementation is the a priori knowledge of the driving cycle, i.e., the driving style of the driver.

In the present work, starting from the optimal ASU mass obtained through the above-mentioned procedure, a control strategy to decide how to split the power between LiBs and SCs is proposed on the basis of a moving average of the power demand. In this way, the driver's behavior is taken into account by the system that optimizes the use of the hybrid storage system predicting the power that will be asked to the storage system. The proposed control strategy was validated by means of numerical simulations. In particular, three EVs were tested on two driving cycles at three different temperatures.

The auxiliary storage unit used was composed of EDLCs because of their good performances in wide temperature ranges. Indeed, even though LiCs have higher energy density than EDLCs, their performances degrade at low temperatures [25]. Indeed, as will be shown, the best improvement due to the presence of the ASU is at low temperatures, when LiBs present bad performances.

3. Proposed Control Algorithm

In this section, the optimal sizing procedure proposed in [24] is briefly reported, and then its real-time implementation is proposed.

3.1. Optimal Sizing Procedure

The sizing procedure proposed in [24] was based on the choice of a driving cycle. For this reason, it was considered that the power demand was known a priori. Given an EV, with its mechanical parameters and the speed profile of the selected driving cycle, the related power profile to be exchanged with the ESS is obtained through the following mechanical equations:

$$p_{dis} = \frac{\left(0.5C_D S\rho v^2 + C_v Mg\cos\alpha + M_e a + Mg\sin\alpha\right)v}{\eta_{dis}}$$
$$p_{cha} = \left(0.5C_D S\rho v^2 + C_v Mg\cos\alpha + M_e a + Mg\sin\alpha\right)v\eta_{cha} \quad (1)$$
$$p_{tot} = p_{dis} + p_{cha}$$

where v and a are the speed and acceleration of the EV, respectively, while α is the slope of the road. The mass (M), equivalent rotational mass (M_e), aerodynamic coefficient (C_D), rolling friction (C_V), and front surface (S) are all characteristic parameters of the chosen EV. ρ is the air density, and g is the gravitational acceleration. Finally, η_{cha} and η_{dis} are, respectively, the total charge and total discharge efficiencies, which depend on both the inverter and the mechanical transmission.

According to the sizing procedure, a certain mass for the auxiliary storage is added to the lithium ion battery pack installed on board. Consequently, the power profile (1) is corrected by also taking into account this additional mass. In order to find the optimal value of the ASU mass, the latter starts from zero (which means only LiBs), and it is iteratively increased, with a chosen fixed mass step, until the maximum value of the ASU mass is reached. For each step, the power profile obtained through (1) can be decomposed as follows:

$$p_{tot} = P_{tot} + p_o \quad (2)$$

where P_{tot} and p_o are, respectively, the constant average value and oscillating part (with zero mean value) of the total power profile (1). The former is related to the energy that is supplied by the ESS and wasted in friction. In contrast, the latter is related to the energy that is exchanged between the ESS and EV.

The basic idea is to use only LiBs to supply the mean value of the power demand, $P_{tot.}$ Moreover, LiBs could also cover a fraction of the oscillating power. An optimization procedure is used to find the optimal fraction of the oscillating power to be covered by the ASU. Therefore, the power exchanged with the ASU, initially supposed to have unitary efficiency, can be calculated as a sub-portion of the oscillating power p_o, which is directly related to the capacity of the ASU, and thus to its mass. Therefore, the value of this mass for which the entire oscillating power p_o is exchanged by the ASU is the maximum one. Instead, the value of the ASU mass that yields the maximum electric vehicle range (EV-R) is the optimal sizing mass, m_o. Consequently, the power portion exchanged by the ASU is proportional to the ratio between the maximum energy variation allowed by the capacity of the ASU, ΔE_{ASU}, which is a function of the additional mass, and the maximum energy variation related to the total power profile (1), ΔE_{max}, as follows:

$$p_{ASU} = p_o \frac{\Delta E_{ASU}}{\Delta E_{max}}. \tag{3}$$

The sizing procedure stops when the mass of the ASU reaches the maximum value, i.e., the value for which p_{ASU} becomes equal to p_o.

Once the power exchanged with the ASU is calculated, the power exchanged with the LiBs is as follows:

$$p_{BAT} = p_{tot} - p_{ASU}. \tag{4}$$

3.2. Real Time Control Strategy Implementation

Once the optimal ASU mass is chosen for an EV, in a real scenario, the power profile p_{tot} is not known a priori. In order to apply the algorithm, it is necessary to estimate the average power P_{tot} by knowing only the actual and past total power profiles. In this paper, we propose to estimate the average power by computing a moving average of the instantaneous power required by the driver. The length of the moving average window is the key parameter of the control strategy that needs to be identified.

Defining the time reference at the beginning of the driving session, the moving average window is implemented as follows:

$$\begin{aligned} P_t &= \frac{1}{t}\int_0^t p_t(x)\,\mathrm{d}x \qquad t \le T_W \\ P_t &= \frac{1}{T_W}\int_{t-T_W}^{t} p_t(x)\,\mathrm{d}x \qquad t > T_W \end{aligned} \tag{5}$$

where p_t is the total instantaneous power required by the traction drive and exchanged with the storage system, P_t is its moving average, and T_W is the window length. The latter will be chosen in order to have the best range extension and will be discussed later. Once P_t is calculated, the control system splits the total required power p_t between the LiBs and ASU as follows:

$$\begin{cases} p_{ASU} = (p_t - P_t)G \\ p_{BAT} = p_t - p_{ASU} \end{cases} \tag{6}$$

where G is the split coefficient and corresponds to the ratio between ΔE_{ASU} and ΔE_{max} of (3):

$$G = \frac{\Delta E_{ASU}}{\Delta E_{max}}. \tag{7}$$

In particular, the value of this coefficient related to the optimal ASU mass found using the procedure reported in the previous section is the optimal split coefficient G_o.

It is worth noting that the power split given by (6) can lead to the full charge or full discharge of the ASU. This is true for two main reasons. First, the ASU does not have unitary efficiency, as supposed in the sizing procedure. Second, the power demand is not known a priori, and the power split is obtained using the moving average defined by (5). In a case where the ASU is fully charged or discharged, the control algorithm will use only the battery.

4. Energy Storage System Models

In order to verify the effectiveness of the proposed control strategy for the hybrid storage system, some numerical simulations were performed. It was necessary to simulate the power exchanged by the storage system with the traction drive throughout the entire EV range. The models used for the simulations had to provide sufficient detail to represent all of the significant phenomena, but they also had to be simple enough to allow long simulations. This was the main principle used to select the models to be used. Some details about the chosen models are given in the following.

4.1. LiB Model

The most diffused electrical battery model consists of a voltage source in series with a resistor and two RC parallel branches. The resistor represents the high frequency resistance of the battery, while the two RC branches model the dynamic response of the battery. For the purposes of this study, the dynamic behavior of the model took into account the relaxation time of the lithium batteries occurring in time ranges from tens of seconds to tens of minutes. For this reason, from a dynamic point of view, the battery was modeled with a resistive branch, R_1, in series with only one parallel RC branch, R_2C_2. In order to represent the behaviors at different temperatures, all of the parameters of the equivalent circuit were variable with the temperature itself. The voltage source, representing the open circuit voltage, was a function of the current and temperature, as well as of the state of discharge (SOD) of the battery pack. In particular, in this study, the model proposed in [2] was used. In this model, the open circuit voltage is split into two voltage sources, one dependent only on the temperature, ΔE, and the other one dependent on an *apparent state of discharge* (ASOD), V_{oc}, taking into account the effects of the current and temperature on the voltage source. The ASOD is defined as follows:

$$ASOD(I,T) = SOD + \alpha(I) + \beta(T)$$

where I is the current exchanged with the battery, T is its temperature, and α and β are parameters depending on the current and temperature, respectively.

According to the procedure proposed in [2], the parameters of the equivalent circuit reported in Fig. 1, for a single 10 Ah lithium ion battery at 8773160 K, were experimentally identified and are reported in Table 1. The dependence of the open circuit voltage on the temperature is represented by a 9th order polynomial function, as follows:

$$V_{oc}(ASOD,) = \sum_{k=0}^{9} p_k ASOD(I,T)^k$$

whose coefficients are reported in Table 2.

The whole battery pack was composed of several cells connected in series and parallel. Based on the hypothesis that all of the cells are equal, the equivalent circuit of the battery pack can be obtained considering the appropriate series and parallel equivalents of the circuit parameters.

4.2. EDLC Model

In the technical literature, several models for EDLCs have been proposed. The most common models are constituted by the series of the main capacitor, whose capacitance is variable with the voltage, the series resistor, and several (theoretically infinite) RC parallel branches representing the dynamic response of the storage device. Moreover, several series RC branches can be connected in parallel to model recombination and self-discharge phenomena [26]. In this paper, self-discharge and recombination are not of interest, and such parallel branches are not considered. Moreover, because the analysis focuses on dynamics ranging from seconds to minutes, the series RC branches can also be neglected. For this reason, in the scope of this study, a simple RC model that considered only the main capacitor and series resistor was used to simulate the EDLC behavior. The capacitance and resistance values are taken from the datasheet of the Maxwell K2 ULTRACAPACITOR 3V/3000F cells. Although, this kind of EDLC has a minimum voltage of 0 V, in this work, it was fixed at 1 V in order to avoid high currents and take into account the technical limits of power converters. The whole EDLC pack is composed of several cells connected in series and in parallel. Based on the hypothesis that all the cells are equal, the equivalent circuit of the EDLC pack can be obtained by considering the appropriate series and parallel equivalents of the circuit parameters.

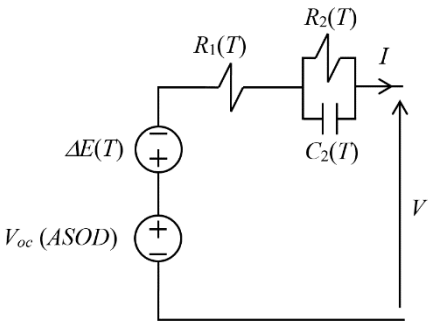

Fig. 1. *Battery model*

Table 1 Parameters of battery cell

Term	Interpolating function
$\alpha(I)$	= -0.1272•exp(-0.1322•I)+0.02807
$\beta(T)$	= 0.1025•exp(-0.08989•T)-0.01953
$\Delta E(T)$	= 0.02552•exp(-0.4304•T)-8.708•10^{-5}
$R_1(T)$	= 0.008472•exp(-0.03645•T)+0.001586
$R_1(T)+R_2(T)$	= 0.0186•exp(-0.04639•T)+0.004498
$C_2(T)$	= 10/$R_2(T)$

Table 2 Coefficients of 9th order polynomial function

Coefficient	
p_0	4.206
p_1	-2.605
p_2	30.81
p_3	-280.7
p_4	1430
p_5	-4261
p_6	7623
p_7	-8056
p_8	4634
p_9	-1119

5. Driving Cycles and EV Parameters

The effectiveness of the proposed control strategy depends, of course, on the driver's behavior and the vehicle on which it is implemented. Therefore, in order to prove its effectiveness, various driving cycles and vehicles had to be considered. In relation to the driving cycles, the NEDC and SC03 were chosen. The NEDC was used because it is the standard on which an EV range is often declared by the OEM. In any case, its speed profile is far from that of a real cycle. For this reason, the second chosen cycle was the SC03. Indeed, even though the SC03 was defined to test the emissions of diesel engines, its speed profile is more similar to a real case.

The driving cycles defined only the vehicle speed profile. In order to test the proposed algorithm, it was necessary to obtain, starting from the speed profile, the power required from the storage system. Considering the efficiency of the whole power train to be constant in both the traction and electric braking phases, the power profile could be obtained through the vehicle data [27] using (1).

In relation to the EVs, in order to cover all of the possible applications, three very different vehicles were considered. The first was a small e-Up! The second, chosen from among medium-size vehicles, was the e-Golf, while the third was the Model S, which is the flagship of Tesla. The main data for these vehicles are reported in Table 3.

Table 3 Parameters of EVs

	e-Up!	e-Golf	Model S
Curb weight [kg]	1139	1510	2108
Max weight [kg]	1500	1960	2590
C_D	0.308	0.27	0.24
S [m^2]	2.09	2.19	2.34
C_V	0.007	0.007	0.01
ρ [kg/m^3]		1.184	
η_{cha}		0.431	
η_{dis}		0.804	
Battery Energy Capacity [kWh]	18.7	24.2	60

The sizing procedure [24] for each EV was applied considering the two driving cycles (NEDC and SC03) at three different temperatures (-10, 0, and 30 °C), and the optimal values for the EDLC mass to be added to the on-board LiB pack are reported in Table 4. Moreover, the EV-R values in

cases with and without the EDLCs are also shown, together with the range extension percentages.

In order to implement the proposed control strategy described in section 3, for each EV, one optimal EDLC mass had to be selected. The vehicle equipped with this ASU was then simulated in all the driving scenarios (different driving cycles at different temperatures). Looking at Table 4, we can recognize that the EDLC mass values obtained in all the cases related to the NEDC driving cycle were between 76 and 137 kg. In contrast, for the SC03 driving cycle, these mass values were between 26 and 49 kg. The latter can be the mass values chosen for each EV because these values correspond to around 10–20% of the battery pack weight, which would be a reasonable choice. In particular, among the different sub-cases at the three temperatures, the values related to the case at 0 °C has been used, because this case is in the middle between low and high temperatures. Furthermore, in order to make a shrewder choice, Fig. 2–Fig. 4 show the behavior of the EV-R as a function of the EDLC mass for each EV related to driving scenario SC03 at 0 °C. Based on an analysis of the figures, it is clear that even if the optimal values are the ones reported in Table 4, it is better to choose lower values that correspond to a slightly lower EV-R. In fact, for example, for the e-Golf, the optimal value for the EDLC mass would be 38 kg, but with 28 kg, practically the same EV-R can be achieved with a lower mass. The masses for the other EVs were chosen following the same approach.

Finally, in order to implement the control strategy and obtain the power demand for the ASU, the split coefficients were calculated accordingly to (7). Table 5 lists the chosen masses and related split coefficients for each EV.

Table 4 Optimal EDLC masses and EV ranges

		m_o [kg]	EV-R LiB [km]	EV-R LiB+ EDLC [km]	Range extension [%]
e-Up!	NEDC -10 °C	100	8.5	119.6	1312%
	NEDC 0 °C	95	141.3	154.1	9.0%
	NEDC 30 °C	89	150.9	154.9	2.6%
	SC03 -10 °C	30	2.9	116.5	3935%
	SC03 0 °C	26	135.3	150.3	11.0%
	SC03 30 °C	28	145.1	151.5	4.4%
e-Golf	NEDC -10 °C	109	9.6	137.1	1323%
	NEDC 0 °C	96	163.4	177.2	8.4%
	NEDC 30 °C	87	173.0	178.2	3.0%
	SC03 -10 °C	37	2.9	126.9	4297%
	SC03 0 °C	35	146.9	163.0	10.9%
	SC03 30 °C	37	157.3	163.8	4.1%
Model S	NEDC -10 °C	137	86.9	256.8	195.7%
	NEDC 0 °C	98	315.8	322.7	2.2%
	NEDC 30 °C	76	317.3	322.9	1.8%
	SC03 -10 °C	47	66.3	236.3	256.4%
	SC03 0 °C	42	279.0	294.3	5.5%
	SC03 30 °C	49	285.0	295.1	3.6%

Table 5 Chosen EDLC masses and split coefficients

	m_o [kg]	G_o
e-Up!	25	0.8323
e-Golf	28	0.7627
Model S	40	0.8146

6. Simulation Results

To test the proposed strategy and identify the best window length (T_W) to ensure the maximum range extension, a Simulink model of the system was implemented. Each of the three vehicles was modeled taking into account the EDLC masses and split coefficients reported in the previous section. Each vehicle was then tested at -10, 0, and 30 °C with the two driving cycles.

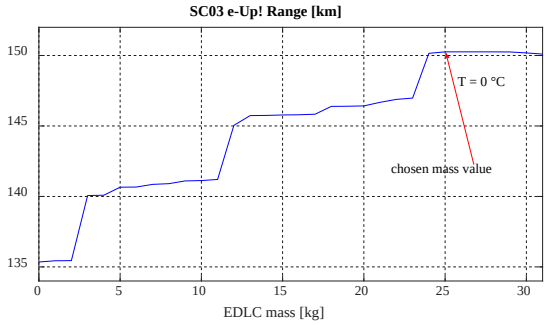

Fig. 2. *EV-R as function of EDLC mass (SC03 – e-Up! at 0 °C)*

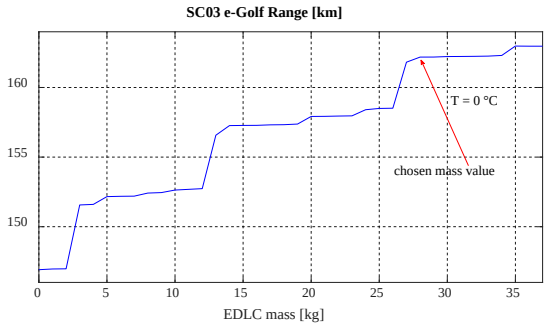

Fig. 3. *EV-R as function of EDLC mass (SC03 – e-Golf at 0 °C)*

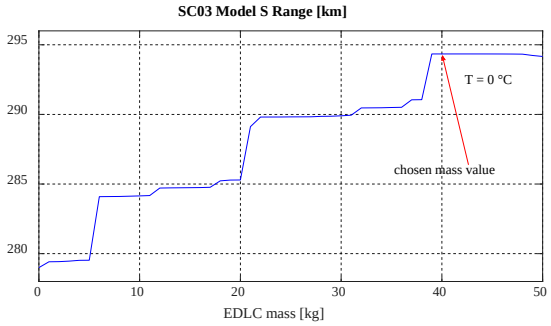

Fig. 4. *EV-R as function of EDLC mass (SC03 – Model S at 0 °C)*

In particular, the three EVs were modeled considering their dynamics using the parameters reported in Table 3. To simulate the driving system response, a suitably tuned PI controller, starting from the reference speed profile provided by the driving cycles and taking into account the charge and discharge efficiencies, generated the required electrical power, pt. This electrical power was then split by the proposed controller into the two contributions p_{BAT} and p_{ASU}, which were input to the LiB and EDLC models, respectively.

Because the main goal of the present work was to analyze some real scenarios in which the driving cycles were not known a priori, the average power of the two driving cycles, NEDC and SC03, was calculated using the moving average defined by (5) with a window length T_W that was different from the periods of the cycles. In order to compare the performances of the real time implementation of the proposed control strategy, for each driving scenario, several simulations were performed by varying the window length of

the moving average between 1 and 20 min in 15 s steps. The case without EDLCs and the case with EDLCs and a priori knowledge of the driving cycle were also included for comparison. The former is referred to as the "base case," and the latter is referred to as the "ideal case" for convenience.

In the simulations, each EV started with both the LiB and EDLC pack fully charged. The vehicle range was calculated by integrating the distance travelled by each EV until the minimum voltage threshold of the LiB, fixed at 2.75 V per cell, was reached.

Fig. 5 shows the calculated range for each EV driven with SC03 and NEDC at -10, 0, and 30 °C. The blue line represents the base case, in which the vehicle did not have EDLCs on board, and the red line represents the ideal case, in which the vehicle has the EDLCs and the control system knows a priori the exact value of the cycle average power. The yellow line is the calculated range for the real case, with different moving average window lengths.

As seen from the NEDC cases, reported in Fig. 5a)–Fig. 5c), with the chosen optimal EDLC mass, no improvement in the range is obtained. This is mainly because the NEDC cycle presents a single strong acceleration near the end of the cycle that brings the vehicle up to 120 km/h. Indeed, because the EDLCs were not dimensioned for this kind of power ripple, the minimum voltage of the LiBs is always reached around that area. Again, for what concerns, in particular, the NEDC case at -10 °C, a small range improvement is obtained with a very short window length, in all cases overcoming the ideal range. Nevertheless, the most consistent NEDC range extension is 12.7%, which is shown by the Model S at -10 °C with a 60 s moving average window. Conversely, for the same vehicle at 30 °C, the extra weight added on board and the extra losses of the system lead to a reduction in the range below the base case.

Fig. 5d)–Fig. 5f) show the calculated range for each EV driven with SC03. In every case, the ASU allows an increase in the vehicle range with respect to the base case. When the moving average is applied to estimate the average power, all of the tests show that there are some window lengths that guarantee a good range extension. Moreover, these tests highlight that for some window lengths, the EV range is even higher than the ideal one. This suggests that, especially when dealing with subzero temperatures, there might be a more suitable control strategy to best exploit the energy available in the lithium batteries.

According to the results reported in Fig. 5, one optimal window length can be selected that is as suitable as possible for almost all of the real cases. Analyzing the results, it is possible to recognize that a window length of 705 s could be a good choice, particularly when looking at the SC03 results that were used to select the EDLC optimal masses. In this way, in all the SC03 cases, the EV range is at least equal to the related ideal case or higher, and for the NEDC cases, the EV range is at least equal to the related base case. Only the Model S shows a slight reduction in the range below the base case. Table 6 reports the EV ranges obtained by applying the proposed control strategy with a moving average window length equal to 705 s.

Table 6 EV-R for optimal window length

EV	Cycle	EV-R LiB [km]	EV-R T_W = 705s [km]	Range extension [%]
e-Up!	SC03 30 °C	145.7	146.9	0.80
	SC03 0 °C	135.3	146.6	8.31
	SC03 -10 °C	2.3	14.4	523.81
	NEDC 30 °C	151.0	151.0	0.00
	NEDC 0 °C	141.4	141.5	0.05
	NEDC -10 °C	8.5	8.5	0.24
e-Golf	SC03 30 °C	157.4	162.3	3.10
	SC03 0 °C	147.0	158.5	7.79
	SC03 -10 °C	2.9	26.0	798.27
	NEDC 30 °C	173.1	173.1	0.01
	NEDC 0 °C	163.5	163.6	0.06
	NEDC -10 °C	9.6	9.6	0.10
Model S	SC03 30 °C	285.0	289.9	1.72
	SC03 0 °C	279.4	289.8	3.72
	SC03 -10 °C	89.3	135.5	51.68
	NEDC 30 °C	317.4	317.2	-0.05
	NEDC 0 °C	315.9	315.8	-0.04
	NEDC -10 °C	86.9	86.9	-0.01

7. Conclusion

EVs are slowly spreading around the world as an alternative solution to traditional vehicles equipped with internal combustion engines. The main limitation to their widespread diffusion is mainly the moderate vehicle range that is possible to reach with the use of energy storage systems. Thanks to the most recent advances in electrochemical storage system technology, i.e., lithium ion batteries, it is possible to travel over 100 km. Nevertheless, this achievable vehicle range is still not comparable to those of traditional vehicles.

This study investigated the use of a hybrid storage system to improve the EV range. In particular, the use of EDLCs with lithium batteries was analyzed. The idea is to use EDLCs to reduce the power peak demand from the batteries and thus improve their efficiency and lifetime. The size of the additional EDLC device was calculated using the results of a previous work, while the power was split between the battery and EDLC using a *split coefficient* defined in the paper.

The evaluation of the optimal split coefficient could be performed based of a knowledge of the driving cycle. However, in a normal application, the driving cycle is not known and, therefore, none of the control strategies based on this knowledge can be used. This paper proposed a new methodology to estimate the split coefficient without knowing the driving cycle. This methodology is based on the measurement of the power demand using a moving average window. The width of this window is a critical parameter of the control strategy, and a value of 705 s was selected based on numerical simulation results.

In order to verify the effectiveness of the proposed control strategy and window width, three EVs with two different driving cycles and three temperatures were simulated.

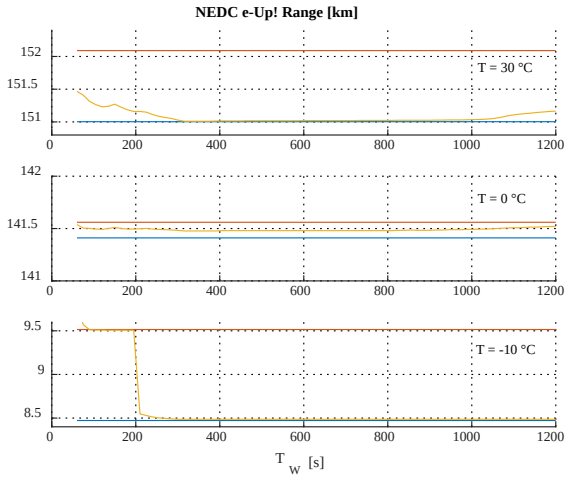

a)

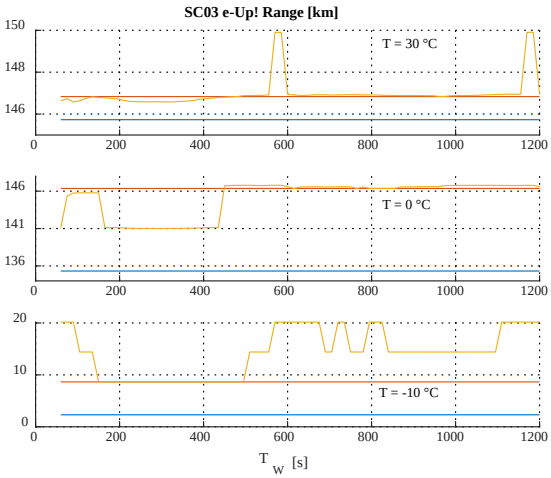

d)

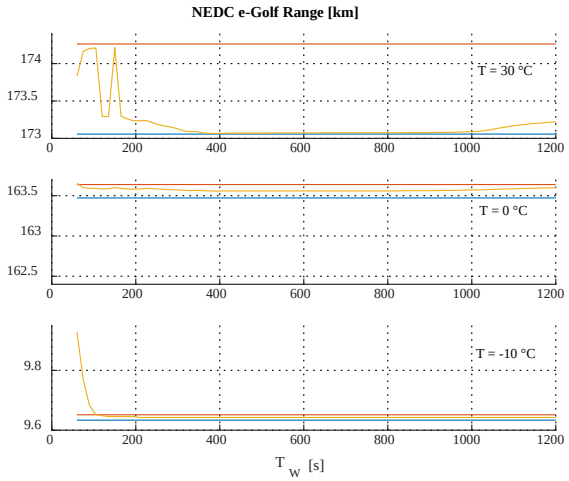

b)

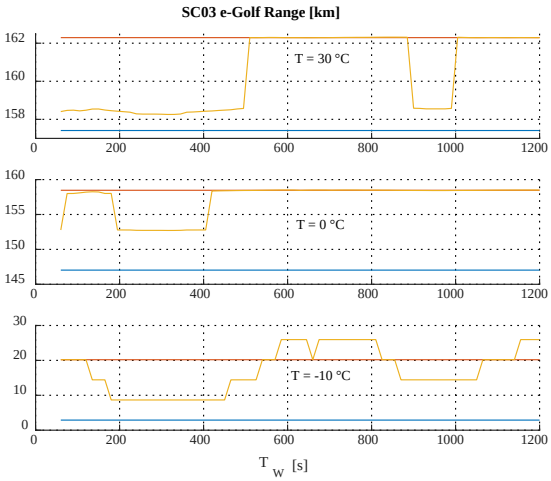

e)

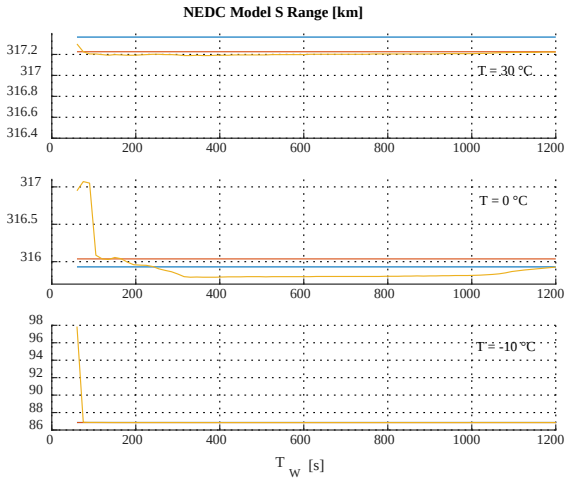

c)

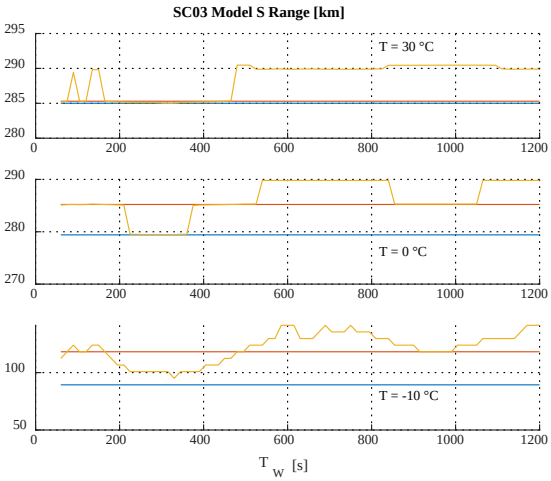

f)

Fig. 5. EV-R as function of window length T_W. Blue line is related to the base case; red line is related to the ideal case; yellow line is related to the real case

The results showed that the introduction of EDLCs controlled by the proposed control strategy brought a substantial range improvement in the cases with a subzero ambient temperature, a condition that is particularly unfavorable to LiBs. Therefore, to enlarge the EV market to cold zones, the use of EDLCs with the proposed control strategy represents a good solution. In future papers, in order to better exploit the effect of the hybrid storage system, the possibility of modifying the vehicle dynamics in terms of the maximum available torque depending on the battery, SOCs, and temperatures [28] will be taken into account. In this way, the peak shaving performed by supercapacitors could be more effective at further reducing the battery stress and improving the vehicle range and battery life.

8. References

[1] Faraj, M., Basir, O.: "Range anxiety reduction in battery-powered vehicles", 2016 IEEE Transportation Electrification Conference and Expo (ITEC), Dearborn, MI, 2016, pp. 1-6

[2] Barcellona, S., Grillo, S., Piegari, L.: "A simple battery model for EV range prediction: Theory and experimental validation", 2016 International Conference on Electrical Systems for Aircraft, Railway, Ship Propulsion and Road Vehicles & International Transportation Electrification Conference (ESARS-ITEC), Toulouse, 2016, pp. 1-7

[3] Fechtner, H., Teschner, T., Schmuelling, B.: "Range prediction for electric vehicles: Real-time payload detection by tire pressure monitoring", 2015 IEEE Intelligent Vehicles Symposium (IV), Seoul, 2015, pp. 767-772

[4] Gebhardt, K., Schau, V., Rossak, W.R.: "Applying stochastic methods for range prediction in E-mobility", 2015 15th International Conference on Innovations for Community Services (I4CS), Nuremberg, 2015, pp. 1-4

[5] Ferreira, J.C., Monteiro, V., Afonso, J.L.: "Dynamic range prediction for an electric vehicle", 2013 World Electric Vehicle Symposium and Exhibition (EVS27), Barcelona, 2013, pp. 1-11

[6] Sautermeister, S., Falk, M., Bäker, B., Gauterin, F., Vaillant, M.: "Influence of Measurement and Prediction Uncertainties on Range Estimation for Electric Vehicles", in IEEE Transactions on Intelligent Transportation Systems, 2018, 19, (8), pp. 2615-2626

[7] Yi, Z., Bauer, P.H.: "Adaptive Multiresolution Energy Consumption Prediction for Electric Vehicles", in IEEE Transactions on Vehicular Technology, 2017, 66, (11), pp. 10515-10525

[8] Miller, J.M., Bohn, T., Dougherty, T.J., Deshpande, U.: "Why hybridization of energy storage is essential for future hybrid, plug-in and battery electric vehicles", 2009 IEEE Energy Conversion Congress and Exposition, San Jose, CA, 2009, pp. 2614-2620

[9] Michalczuk, M., Grzesiak, L.M., Ufnalski, B., "Experimental parameter identification of battery-ultracapacitor energy storage system", 2015 IEEE 24th International Symposium on Industrial Electronics (ISIE), Buzios, 2015, pp. 1260-1265

[10] Ceraolo, M., Giglioli, R., Lutzemberger, G., Sani, L.: "Hybrid energy systems in mobility applications" 2016 AEIT International Annual Conference (AEIT), Capri, 2016, pp. 1-6

[11] Dougal, R.A., Liu, S., White, R.E.: "Power and life extension of battery-ultracapacitor hybrids", in IEEE Transactions on Components and Packaging Technologies, 2002, 25, (1), pp. 120-131

[12] Pay, S., Baghzouz, Y.: "Effectiveness of battery-supercapacitor combination in electric vehicles", 2003 IEEE Bologna Power Tech Conference Proceedings, pp. 6, Vol. 3, 2003.

[13] Khaligh, A., Li, Z.: "Battery, Ultracapacitor, Fuel Cell, and Hybrid Energy Storage Systems for Electric, Hybrid Electric, Fuel Cell, and Plug-In Hybrid Electric Vehicles: State of the Art", in IEEE Transactions on Vehicular Technology, 2010, 59, (6), pp. 2806-2814

[14] Hredzak, B., Agelidis, V.G., Jang, M.: "A Model Predictive Control System for a Hybrid Battery-Ultracapacitor Power Source", in IEEE Transactions on Power Electronics, 2014, 29, (3), pp. 1469-1479

[15] Ostadi, A., Kazerani, M.: "A Comparative Analysis of Optimal Sizing of Battery-Only, Ultracapacitor-Only, and Battery–Ultracapacitor Hybrid Energy Storage Systems for a City Bus", in IEEE Transactions on Vehicular Technology, 2015, 64, (10), pp. 4449-4460

[16] Shen, J., Dusmez, S., Khaligh, A.: "Optimization of Sizing and Battery Cycle Life in Battery/Ultracapacitor Hybrid Energy Storage Systems for Electric Vehicle Applications", in IEEE Transactions on Industrial Informatics, 2014, 10, (4), pp. 2112-2121

[17] Zheng, J., Jow, T., Ding, M.: "Hybrid power sources for pulsed current applications", IEEE Trans. Aerosp. Electron. Syst., 37, (1), 2001, pp. 288-292

[18] Pagano, M. Piegari, L.: "Hybrid electrochemical power sources for onboard applications", IEEE. Trans. Energy Convers., 22, (2), 2007, pp. 450-456

[19] Song, Z., Hofmann, H., Li, J., Han, X., Zhang, X., Ouyang, M.: "A comparison study of different semi-active hybrid energy storage system topologies for electric vehicles" J. Power Sources, 274, 2015, pp. 400-411

[20] Zhang, L., Hu, X., Wang, Z., Sun, F., Deng, J., Dorrell, D.G.: "Multiobjective Optimal Sizing of Hybrid Energy Storage System for Electric Vehicles," in IEEE Transactions on Vehicular Technology, 67, (2), 2018, pp. 1027-1035

[21] Camara, M.B., Gualous, H., Gustin, F., Berthon, A.: "DC/DC converter design for supercapacitor and battery power management in hybrid vehicle applications—Polynomial control strategy", IEEE Trans. Ind. Electron., 57, (2), 2010, pp. 587-597

[22] Parwal, A., Fregelius, M., Temiz, I., Göteman, M., de Oliveira, J.G., Boström, C., Leijon, M.: "Energy management for a grid-connected wave energy park through a hybrid energy storage system", Applied Energy, 231, 2018, pp. 399-411

[23] Amjadi, Z., Williamson, S.S.: "Power-Electronics-Based Solutions for Plug-in Hybrid Electric Vehicle Energy Storage and Management Systems," in IEEE Transactions on Industrial Electronics, 57, (2), 2010, pp. 608-616

[24] Barcellona, S., Piegari, L.: "Improvement of EVs Range by Hybrid Storage Units", 2017 IEEE Vehicle Power and Propulsion Conference (VPPC), Belfort, 2017, pp. 1-5

[25] Barcellona, S., Piegari, L.: “A lithium-ion capacitor model working on a wide temperature range”, Journal of Power Sources, 2017, 342, pp. 241-251

[26] Musolino, V., Piegari, L., Tironi, E.: "New Full-Frequency-Range Supercapacitor Model With Easy Identification Procedure", IEEE Transactions on Industrial Electronics, 2013, 60, (1), pp.112-120

[27] Grunditz, E.A., Thiringer, T.: "Performance Analysis of Current BEVs Based on a Comprehensive Review of Specifications", in IEEE Transactions on Transportation Electrification, 2016, 2, (3), pp. 270-289

[28] Galdi, V., Piccolo, A., Siano, P.: "A Fuzzy Based Safe Power Management Algorithm for Energy Storage Systems in Electric Vehicles," 2006 IEEE Vehicle Power and Propulsion Conference, Windsor, 2006, pp. 1-6.